Biogeosciences Discuss., 8, 10229–10246, 2011
www.biogeosciences-discuss.net/8/10229/2011/
doi:10.5194/bgd-8-10229-2011

Biogeosciences Discussions

Sea-to-air and diapycnal nitrous oxide fluxes in the eastern tropical North Atlantic Ocean

A. Kock[1], J. Schafstall[2], M. Dengler[2], P. Brandt[2], and H. W. Bange[1]

[1]Forschungsbereich Marine Biogeochemie, IFM-GEOMAR, Leibniz-Institut für Meereswissenschaften, Düsternbrooker Weg 20, 24105 Kiel, Germany
[2]Forschungsbereich Ozeanzirkulation und Klimadynamik, IFM-GEOMAR, Leibniz-Institut für Meereswissenschaften, Düsternbrooker Weg 20, 24105 Kiel, Germany

Received: 12 October 2011 – Accepted: 13 October 2011 – Published: 20 October 2011

Correspondence to: A. Kock (akock@ifm-geomar.de)

Published by Copernicus Publications on behalf of the European Geosciences Union.

Abstract

Sea-to-air and diapycnal fluxes of nitrous oxide (N_2O) into the mixed layer were determined during three cruises to the upwelling region off Mauritania. Both fluxes were elevated close to the shelf break, but elevated sea-to-air fluxes reached further offshore as a result of the offshore transport of upwelled water masses. To calculate a mixed layer budget for N_2O we compared the regionally averaged sea-to-air and diapycnal fluxes and estimated the potential contribution of other processes, such as vertical advection and biological N_2O production in the mixed layer. Using common parameterizations for the gas transfer velocity, the comparison of the average sea-to-air and diapycnal N_2O fluxes indicated that the mean sea-to-air flux is about three to four times larger than the diapycnal flux. Vertical and horizontal advection or biological production were found not sufficient to close the mixed layer budget. Instead, the sea-to-air flux, calculated using a parameterization that takes into account the attenuating effect of surfactants on gas exchange, is in the same range as the diapycnal flux. This indicates that common parameterizations for the gas transfer velocity might overestimate the air-sea gas exchange within highly productive upwelling zones.

1 Introduction

Nitrous oxide (N_2O) is a potent greenhouse gas with a major contribution of oceanic emissions to its atmospheric budget (Denman et al., 2007). It is produced in the oxic subsurface and deep ocean during microbial nitrification, whereas in anoxic to suboxic parts of the ocean N_2O can be produced and/or consumed during canonical denitrification (see e.g. Bange et al., 2010). While large parts of the surface ocean are close to equilibrium with the atmosphere, enhanced emissions are observed during coastal upwelling events due to the transport of N_2O-enriched subsurface waters into the mixed layer (ML, see e.g. Nevison et al., 2004). Pronounced coastal upwelling in the eastern tropical North Atlantic Ocean (ETNA) occurs seasonally along the coasts

BGD
8, 10229–10246, 2011

of Mauritania and Senegal. Consistently, N_2O emissions are found to be enhanced during winter/spring (Wittke et al., 2010).

In this study we quantify the diapycnal and sea-to-air fluxes of N_2O in the ETNA (incl. the upwelling off Mauritania) to estimate the contribution of diapycnal mixing to the N_2O ML budget: N_2O concentrations in the ML should, at steady state, represent the balance between physical processes such as vertical mixing, air-sea gas exchange with the overlying atmosphere, vertical and horizontal advection and biological processes such as nitrification. The relative importance of the different terms for the N_2O ML budget is discussed. It is found that diapycnal and sea-to-air fluxes are the leading terms in the N_2O ML budget and sea-to-air fluxes are likely overestimated when using common parameterizations for the gas transfer velocity.

1.1 Study site

The investigated area covers the ETNA between the Cape Verde Islands and coast of Mauritania (Fig. 1). A lack of river inputs combined with a narrow continental shelf minimizes additional contributions of N_2O originating from riverine or sedimentary sources. The Mauritanian upwelling system is the most productive southern branch of the Canary Current upwelling system (Minas et al., 1982; Signorini et al., 1999), showing a seasonality which follows the shifting of the Inter-Tropical Convergence Zone (ITCZ) throughout the year (Hagen, 2001). In the region between Cap Vert (~15° N) and Cap Blanc (~21° N) seasonal upwelling takes place during winter/spring (Schemainda et al., 1975). Compared to other eastern boundary upwelling systems, the water column in the ETNA has relatively high oxygen concentrations: minimum oxygen concentrations reach down to 40 µmol L^{-1} (Stramma et al., 2008). We thus conclude that the main production pathway for N_2O in this region is nitrification.

BGD
8, 10229–10246, 2011

2 Methods

N_2O concentration, microstructure and conductivity-temperature-depth (CTD) measurements were conducted during three cruises to the ETNA (Fig. 1). The cruises were part of the German BMBF joint project SOPRAN (Surface Ocean Processes in the Anthropocene, www.sopran.pangaea.de) and the DFG-funded Mauritanian upwelling and mixing process study (MUMP). They were scheduled in the upwelling season in January/February 2007 (R/V *Poseidon* cruises P347 and P348) and February 2008 (R/V *L'Atalante* cruise ATA3). Triplicate water samples taken from the CTD/rosette casts were analyzed for dissolved N_2O on board using a GC/ECD system with a static equilibration method. For details of the method see Walter et al. (2006). The average precision of the measurements, calculated from error propagation, was $\pm 0.7\,\mathrm{nmol\,L^{-1}}$.

N_2O sea-to-air fluxes F_{sta} (in $\mathrm{nmol\,m^{-2}\,s^{-1}}$) were calculated from the gas exchange equation:

$$F_{sta} = k_w \Delta N_2O = k_w \times ([N_2O]_w - [N_2O]_a) \quad (1)$$

where k_w is the gas transfer velocity and $[N_2O]_w$ is the measured in-situ concentration from the shallowest Niskin bottle in the surface layer (5–10 m). The N_2O equilibrium concentration $[N_2O]_a$ was calculated by using a mean dry mole fraction of 321 ppb (extracted from the monthly time series of atmospheric N_2O from the AGAGE monitoring station Ragged Point on Barbados, see http://agage.eas.gatech.edu, Prinn et al., 1990) and the temperature and salinity at the depth of the corresponding Niskin bottle. k_w was calculated using the k_w/wind speed relationships as defined by Nightingale et al. (2000), Liss and Merlivat (1986) and Wanninkhof (1992). Wind speeds were obtained from the ships' underway observations. Alternatively, the sea-to-air flux densities were calculated using the gas transfer velocity parameterization from Tsai and Liu (2003) that takes into account the reduction of the air-sea gas exchange due to surfactants.

Ocean turbulence profiles were obtained by using microstructure profilers (MSS) as described in details by Schafstall et al. (2010). Briefly, the MSS are loosely-tethered

BGD
8, 10229–10246, 2011

profilers that measure small-scale velocity fluctuations from which the dissipation rate of turbulent kinetic energy (ε) is determined. To estimate the diapycnal N_2O fluxes into the ML we used the station-average diapycnal diffusivities derived from microstructure measurements from 5 m below the ML depth to the depth of the next deeper N_2O water sample. The ML depth at individual stations was determined using the density criterion described by Kara et al. (2000). To avoid any influence from turbulence caused by the ship, the minimum ML depth was set to be at least 15 m deep. The diapycnal diffusivity K_ρ was computed according to Osborn (1980) as

$$K_\rho = \Gamma \frac{\varepsilon}{N^2}, \tag{2}$$

and diapycnal fluxes F_{dia} of N_2O as

$$F_{\text{dia}} = K_\rho \cdot \frac{d[\text{N}_2\text{O}]}{dz}, \tag{3}$$

with the local buoyancy frequency N and the mixing efficiency Γ which was set to a constant value of 0.2 (Oakey, 1982) and the concentration gradient $d[\text{N}_2\text{O}]/dz$. Fluxes were determined only from those microstructure profiles which were recorded concurrently with N_2O profile sampling.

3 Results and discussion

To illustrate the N_2O sea-to-air and diapycnal fluxes, the point estimates were projected onto the distribution of topography along 18° N (Fig. 2). This procedure implicitly assumes that the mean fluxes have larger cross-shore than along-shore gradients (Schafstall et al., 2010).

The N_2O sea-to-air fluxes using the Nightingale et al. (2000) parameterization ranged from −0.02 to 0.5 nmol m^{-2} s^{-1} (Fig. 2). Highest fluxes were found close to the shelf break in the zone of active upwelling indicated by low sea surface temperatures (SST).

BGD
8, 10229–10246, 2011

N_2O sea-to-air fluxes decreased with distance from the shelf break, which can be explained by a combination of continuous outgassing from N_2O-enriched waters and its offshore transport within cold filaments.

The open ocean sea-to-air fluxes (west of 18° W) are in agreement with the fluxes computed by Walter et al. (2006). The coastal fluxes between 18° and 16° W are, despite resulting from a different approach, in reasonable agreement with the model-adjusted sea-to-air fluxes computed by Wittke et al. (2010). The majority of the fluxes are positive indicating a flux of N_2O from the ocean to the atmosphere. However, we also computed negative fluxes which denote a N_2O flux from the atmosphere into the ocean. These negative fluxes correspond to ΔN_2O values of max. $-0.3\,\mathrm{nmol\,L^{-1}}$ and are therefore within the uncertainty range of the measurements.

The majority of the diapycnal N_2O fluxes were lower than the N_2O sea-to-air fluxes from the Nightingale et al. (2000) parameterization. Largest diapycnal fluxes were found in a narrow band at the shelf break. However, enhanced fluxes were also encountered at the shelf. Since the vertical N_2O gradients were rather uniform, the variability of diapycnal fluxes is predominately due to the variability of diapycnal diffusivities (K_ρ) that were greatly enhanced towards the shelf break (Schafstall et al., 2010).

To determine regional averages of the N_2O sea-to-air fluxes, the point estimates were extrapolated exploiting the dependence of surface ΔN_2O on SST anomaly (Fig. 3a). For this we used eight day mean MODIS Aqua SST data (http://oceandata.sci.gsfc.nasa.gov/MODISA/Mapped/8Day/4km/SST/) that covered the sampling periods.

The calculations were performed for an upwelling box off the Mauritanian coast. The size of the box was defined by the northernmost and southernmost sampled station, that is 20°10′ N and 16°10′ N respectively, the Mauritanian coastline (except the Banc D'Arguin with bottom depths <10 m) and a line parallel to the shelf break located 170 km offshore. The SST anomaly was defined as the difference between the SST at a respective position in the upwelling box and the background SST averaged along a 100 km long section to the west of the box, thereby taking into account its mean latitudinal dependence.

BGD
8, 10229–10246, 2011

Negative SST anomalies (SSTA) were significantly correlated with ΔN_2O (r^2 = 0.54, n = 45; Fig. 3). A linear regression was used to calculate the regional surface ΔN_2O distribution from the SSTA (ΔN_2O = C*SSTA, with C = −2.82 nmol L^{-1} °C^{-1}). ΔN_2O values from positive SST anomalies were set to zero, assuming that these values were not influenced by upwelling. The corresponding N_2O sea-to air fluxes, calculated with the Nightingale (2000) parameterization, were calculated from three day mean QuikScat wind speeds (ftp://ftp.ssmi.com/qscat/bmaps_v03a/) (Fig. 5a). The resulting flux, averaged over the sampling period and the upwelling box, were 0.0685 (0.0677 to 0.0693) nmol m^{-2} s^{-1}. The confidence intervals were calculated using a Monte Carlo simulation with the uncertainties of the ΔN_2O calibration and an assumed uncertainty of ±2 m s^{-1} for the wind speed as input variables. To account for the large uncertainties in gas exchange velocities, we additionally calculated sea-to-air fluxes using the gas exchange parameterizations by Liss and Merlivat (1986) and Wanninkhof (1992) as lower and upper boundaries (Wanninkhof et al., 2009) (Table 1).

In contrast to the sea-to-air fluxes, the diapycnal fluxes were averaged in two regions according to their water depths: the shelf (water depth <400 m) and open ocean (water depth ≥400 m) region (Fig. 4). The average fluxes were 0.07 (0.025 to 0.126) nmol m^{-2} s^{-1} for the shelf and 0.004 (0.002 to 0.007) nmol m^{-2} s^{-1} for the open ocean region (Fig. 5b). This results in an overall average flux of 0.019 (0.007 to 0.048) nmol m^{-2} s^{-1}. Confidence intervals were calculated from error propagation, as detailed in Schafstall et al. (2010).

Although the diapycnal flux estimate shows large uncertainties and the calculated sea-to-air flux strongly depends on the choice of the gas exchange parameterization, the comparison of the sea-to-air fluxes with the diapycnal flux shows a large discrepancy between the two fluxes. None of the commonly used gas exchange parameterizations is able to adequately close the discrepancy, with the average diapycnal flux only explaining about 25–30 % of the average sea-to-air flux determined from the Nightingale et al. (2000) parameterization.

BGD
8, 10229–10246, 2011

The missing oceanic flux required to close the N_2O ML budget cannot be attributed to vertical advection of N_2O resulting from Ekman divergence, however. A regional average of the vertical advective flux (F_{adv}) calculated from wind stress curl using QuikSCAT winds and N_2O concentration differences between the ML and the next deeper available value, from 10 to 30 m below the ML, resulted in 0.0021 nmol m^{-2} s^{-1} (Schafstall, 2010). Vertical advection of N_2O is thus nearly an order of magnitude lower than the diapycnal flux. Similarly, the horizontal flux divergence associated with a mean N_2O gradient along the eastern boundary current is not able to close the N_2O ML budget.

N_2O production from near-surface nitrification has been previously suggested to close the discrepancy between diapycnal and sea-to-air fluxes (e.g., Dore and Karl (1996); Santoro et al., 2010). Recent publications have shown that nitrification within the euphotic zone can play a significant role in nutrient cycling of the surface ocean (Clark et al., 2008; Santoro et al., 2010; Wankel et al., 2007; Yool et al., 2007).

Based on the estimates of diapycnal, advective and sea-to-air flux we calculated potential N_2O production rates closing the N_2O ML budget, assuming a ML depth of 25 m (Table 1). Although covering a large range, the calculated N_2O production rates are extremely high: Using the Nightingale (2000) parameterization, the average N_2O ML production rate must be as high as about 60 nmol kg^{-1} yr^{-1} (0.16 nmol L^{-1} d^{-1}). This exceeds N_2O production rates in the water column below the ML, quantified to be $\leq$3.2 nmol kg^{-1} yr^{1} (Freing, 2009), by far. With a molar N_2O yield during nitrification between 0.5 and 0.01 % (Bange, 2008) the corresponding nitrification rates would range from 30 to 1500 nmol L^{-1} d^{-1}. This is significantly higher than the nitrification rates of up to 5 nmol L^{-1} d^{-1} from ML samples from Mauritanian upwelling region measured by Clark et al. (2008) which, for comparison, would yield an N_2O flux of 0.001 nmol m^{-2} s^{-1} at a N_2O yield of 0.1 %.

The ML budget could yet be closed using a gas exchange parameterization that takes into account the attenuating effect of surfactants on air-sea gas exchange (Tsai and Liu, 2003). The resulting average sea-to-air flux for the upwelling box is 0.020 nmol m^{-2} s^{-1} and thus of similar magnitude as the diapycnal flux (Table 1,

BGD
8, 10229–10246, 2011

Fig. 5c). SeaWiFs chlorophyll images (not shown) indicate that the investigated area was highly productive during the sampling periods, which in general has been associated with the occurrence of surface slicks (Lin et al., 2002; Wurl et al., 2011). However, the Tsai and Liu (2003) parameterization only represents a simplified approach that attributes the occurrence of surfactants with a very large reduction of air-sea gas exchange. Quantitative estimates of the surfactant effects on gas exchange reveal large uncertainties, and most field studies report smaller effects of surfactants on gas exchange (Schmidt and Schneider, 2011; Upstill-Goddard, 2006). A more quantitative understanding of the role of surfactants in reducing the air-sea gas exchange would require dedicated studies to evaluate different physical and biogeochemical dependencies.

4 Summary and conclusions

For the first time, microstructure measurements were used to estimate the diapycnal flux of nitrous oxide into the ML. The comparison with sea-to-air fluxes shows a different regional distribution due to the offshore transport of the supersaturated surface waters. The regionally integrated average sea-to-air fluxes using standard parameterizations exceed the average diapycnal flux by a factor of three to four. We argue that this discrepancy is unlikely to be explained by biological N_2O production in the mixed layer or vertical advection alone. Instead, a significantly reduced gas exchange due to the occurrence of surfactants may be a plausible explanation, although there is no direct evidence for a correlation between surfactants and reduced N_2O fluxes so far. Our results indicate that neglecting the surfactant effect on air-sea gas exchange may lead to a significant overestimation of the oceanic emissions of N_2O and other trace gases in highly productive areas.

BGD
8, 10229–10246, 2011

Acknowledgements. We thank the captains and crews of R/V *L'Atalante* and R/V *Poseidon* for their excellent support during the cruises. Also, we thank A. Freing for inspiring discussions about the N_2O mixed layer source and A. Körtzinger, B. Fiedler, T. Tanhua, and M. Glessmer for their support during the field work. Financial support for this study was provided by DFG grants DE 1369/1-1 and DE 1369/3-1 (JS and MD) and BMBF grant SOPRAN FKZ 03F0462A (AK). QuikScat data are produced by Remote Sensing Systems and sponsored by the NASA Ocean Vector Winds Science Team. Data are available at www.remss.com.

References

Bange, H. W.: Gaseous nitrogen compounds (NO,N2O,N2,NH3) in the ocean, in: Nitrogen in the Marine Environment, 2 Edn., edited by: Capone, D. G., Bronk, D. A., Mulholland, M. R., and Carpenter, E. J., Academic Press/Elsevier 51–94, 2008.

Bange, H. W., Freing, A., Kock, A., and Löscher, C. R.: Marine pathways to nitrous oxide, in: Nitrous Oxide and Climate Change, edited by: Smith, K., Earthscan, London, 36–62, 2010.

Clark, D. R., Rees, A. P., and Joint, I.: Ammonium regeneration and nitrification rates in the oligotrophic Atlantic Ocean: Implications for new production estimates, Limnol. Oceanogr., 53, 52–62, 2008.

Denman, K. L., Brasseur, G., Chidthaisong, A., Ciais, P., Cox, P. M., Dickinson, R. E., Hauglustaine, D., Heinze, C., Holland, E., Jacob, D., Lohmann, U., Ramachandran, S., Leite da Silva Dias, P., Wofsy, S. C., and Zhang, X.: Couplings between changes in the climate system and biogeochemistry, in: Climate Change 2007: The Physical Science Basis. Contribution of Working Group I to the Fourth Assessment Report of the Intergovernmental Panel on Climate Change, edited by: Solomon, S., Cambridge University Press, Cambridge, UK and New York, NY, USA, 499–588, 2007.

Dore, J. E. and Karl, D. M.: Nitrification in the euphotic zone as a source for nitrite, nitrate, and nitrous oxide at Station ALOHA, Limnol. Oceanogr., 41, 1619–1628, 1996.

Freing, A.: Production and emissions of oceanic nitrous oxide, PhD, RD-2 Chemical Oceanography, Christian-Albrechts-Universität, Kiel, 128 pp., 2009.

Hagen, E.: Northwest African upwelling scenario, Oceanologica Acta, 24, S113–S127, 2001.

Kara, A. B., Rochford, P. A., and Hurlburt, H. E.: An optimal definition for ocean mixed layer depth, J. Geophys. Res., 105, 16803–16821, 2000.

BGD

8, 10229–10246, 2011

Lin, I. I., Wen, L. S., Liu, K. K., Tsai, W. T., and Liu, A. K.: Evidence and quantification of the correlation between radar backscatter and ocean colour supported by simultaneously acquired in situ sea truth, Geophys. Res. Lett., 29, 1464, doi:10.1029/2001gl014039, 2002.
Liss, P. S. and Merlivat, L.: Air-sea exchange rates: introduction and synthesis, in: The role of air-sea exchange in geochemical cycling, edited by: Buat-Ménard, P., Series C: Mathem. and Phys. Sciences, D. Reidel Publishing Company, Dordrecht, 113–127, 1986.
Minas, H. J., Codispoti, L. A., and Dugdale, R. C.: Nutrients and primary production in the upwelling region off Northwest Africa, Rapports et Procès-Verbaux des Réunions, Conseil International pour L'Exploration de la Mer, 180, 148–182, 1982.
Nevison, C. D., Lueker, T. J., and Weiss, R. F.: Quantifying the nitrous oxide source from coastal upwelling, Global Biogeochem. Cycles, 18, GB1018, doi:10.1029/2003GB002110, 2004.
Nightingale, P., Malin, G., Law, C. S., Watson, A. J., Liss, P. S., Liddicoat, M. I., Boutin, J., and Upstill-Goddard, R. C.: In situ evaluation of air-sea gas exchange parameterizations using novel conservative and volatile tracers, Global Biogeochem. Cycles, 14, 373–387, 2000.
Oakey, N. S.: Determination of the rate of dissipation of turbulent energy from simultaneous temperature and velocity shear microstructure measurements, J. Phys. Oceanogr., 12, 256–271, 1982.
Osborn, T. R.: Estimates of the local-rate of vertical diffusion from dissipation measurements, J. Phys. Ocean., 10, 83–89, 1980.
Prinn, R., Cunnold, D., Rasmussen, R., Simmonds, P., Alyea, F., Crawford, A., Fraser, P., and Rosen, R.: Atmospheric emissions and trends of nitrous-oxide deduced from 10 years of ALE-GAUGE data, J. Geophys. Res.-Atmos., 95, 18369–18385, 1990.
Santoro, A. E., Casciotti, K. L., and Francis, C. A.: Activity, abundance and diversity of nitrifying archaea and bacteria in the central California Current, Environ. Microbiol., 12, 1989–2006, doi:10.1111/j.1462-2920.2010.02205.x, 2010.
Schafstall, J.: Turbulente Vermischungsprozesse und Zirkulation im Auftriebsgebiet vor Nordwestafrika, PhD, RD1 - Physical Oceanography, Christian-Albrechts-Universität, Kiel, 219 pp., 2010.
Schafstall, J., Dengler, M., Brandt, P., and Bange, H.: Tidal-induced mixing and diapycnal nutrient fluxes in the Mauritanian upwelling region, J. Geophys. Res.-Oceans, 115, C10014, doi:10.1029/2009jc005940, 2010.
Schemainda, R., Nehring, D., and Schulz, S.: Ozeanologische Untersuchungen zum Produktionspotential der nordwestafrikanischen Wasserauftriebsregion 1970–1973, Akademie der

BGD
8, 10229–10246, 2011

Wissenschaften der Deutschen Demokratischen Republik, Berlin, 1–88, 1975.
Schmidt, R. and Schneider, B.: The effect of surface films on the air-sea gas exchange in the Baltic Sea, Mar. Chem., 126, 56–62, 2011.
Signorini, S. R., Murtugudde, R. G., McClain, C. R., Christian, J. R., Picaut, J., and Busalacchi, A. J.: Biological and physical signatures in the tropical and subtropical Atlantic, J. Geophys. Res.-Oceans, 104, 18367–18382, 1999.
Stramma, L., Brandt, P., Schafstall, J., Schott, F., Fischer, J., and Kortzinger, A.: Oxygen minimum zone in the North Atlantic south and east of the Cape Verde Islands, J. Geophys. Res.-Oceans, 113, C04014, doi:10.1029/2007jc004369, 2008.
Tsai, W. T. and Liu, K. K.: An assessment of the effect of sea surface surfactant on global atmosphere-ocean CO2 flux, J. Geophys. Res.-Oceans, 108, 3127, doi:10.1029/2000jc000740, 2003.
Upstill-Goddard, R. C.: Air-sea gas exchange in the coastal zone, Estuar. Coast. Shelf Sci., 70, 388–404, doi:10.1016/j.ecss.2006.05.043, 2006.
Walter, S., Bange, H. W., Breitenbach, U., and Wallace, D. W. R.: Nitrous oxide in the North Atlantic Ocean, Biogeosciences, 3, 607–619, doi:10.5194/bg-3-607-2006, 2006.
Wankel, S. D., Kendall, C., Pennington, J. T., Chavez, F. P., and Paytan, A.: Nitrification in the euphotic zone as evidenced by nitrate dual isotopic composition: Observations from Monterey Bay, California, Global Biogeochem. Cyc., 21, Gb2009, doi:10.1029/2006gb002723, 2007.
Wanninkhof, R.: Relationship between wind speed and gas exchange over the ocean, J. Geophys. Res.-Oceans, 97, 7373–7382, 1992.
Wanninkhof, R., Asher, W. E., Ho, D. T., Sweeney, C., and McGillis, W. R.: Advances in Quantifying Air-Sea Gas Exchange and Environmental Forcing, Annu. Rev. Mar. Sci., 1, 213–244, doi:10.1146/annurev.marine.010908.163742, 2009.
Wittke, F., Kock, A., and Bange, H. W.: Nitrous oxide emissions from the upwelling area off Mauritania (NW Africa), Geophys. Res. Lett., 37, L12601, doi:10.1029/2010gl042442, 2010.
Wurl, O., Wurl, E., Miller, L., Johnson, K., and Vagle, S.: Formation and global distribution of sea-surface microlayers, Biogeosciences, 8, 121–135, doi:10.5194/bg-8-121-2011, 2011.
Yool, A., Martin, A. P., Fernandez, C., and Clark, D. R.: The significance of nitrification for oceanic new production, Nature, 447, 999–1002, doi:10.1038/nature05885, 2007.

BGD
8, 10229–10246, 2011

Table 1. Sea-to-air fluxes (F_{sta}) of N_2O calculated with different gas exchange parameterizations and corresponding N_2O production rates at a ML depth of 25 m required to compensate the discrepancy between the sea-to-air flux and the sum of diapycnal (F_{dia}) and vertical advective (F_{adv}) flux.

Parameterization	F_{sta} [nmol m^{-2} s^{-1}]	$F_{sta} - (F_{dia} + F_{adv})$ [nmol m^{-2} s^{-1}]	Required N_2O production rate [nmol L^{-1} yr^{-1}]
Nightingale (2000)	0.0685 (0.0677 to 0.0693)	0.048 (0.018 to 0.060)	61 (22 to 76)
Liss and Merlivat (1986)	0.0461 (0.0455 to 0.0467)	0.026 (−0.005 to 0.038)	33 (−6 to 47)
Wanninkhof (1992)	0.0836 (0.0825 to 0.0846)	0.064 (0.032 to 0.076)	80 (41 to 95)
Tsai and Liu (2003)	0.0198 (0.0195 to 0.0201)	−0.001 (−0.031 to 0.011)	−1 (−40 to 14)

BGD
8, 10229–10246, 2011

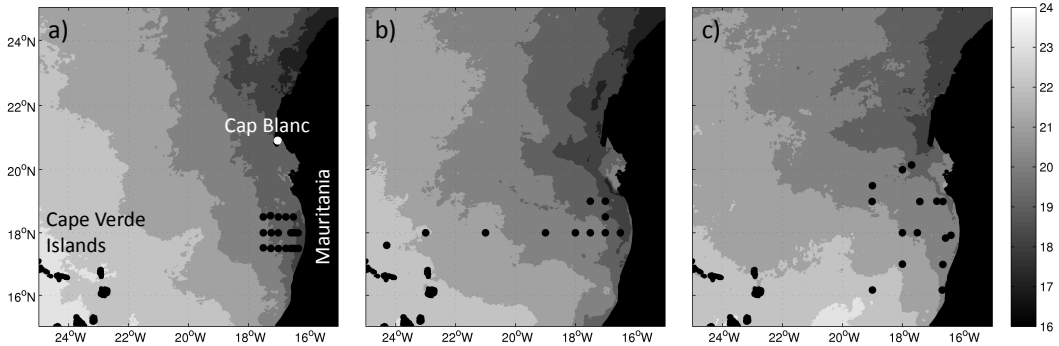

Fig. 1. Map with locations of the sampled stations during P347 in January 2007 **(a)**, P348 in February 2007 **(b)** and ATA3 in February 2008 **(c)**. MODIS monthly sea surface temperatures (in ˚C) are also shown (http://oceandata.sci.gsfc.nasa.gov/MODISA/Mapped/).

BGD
8, 10229–10246, 2011

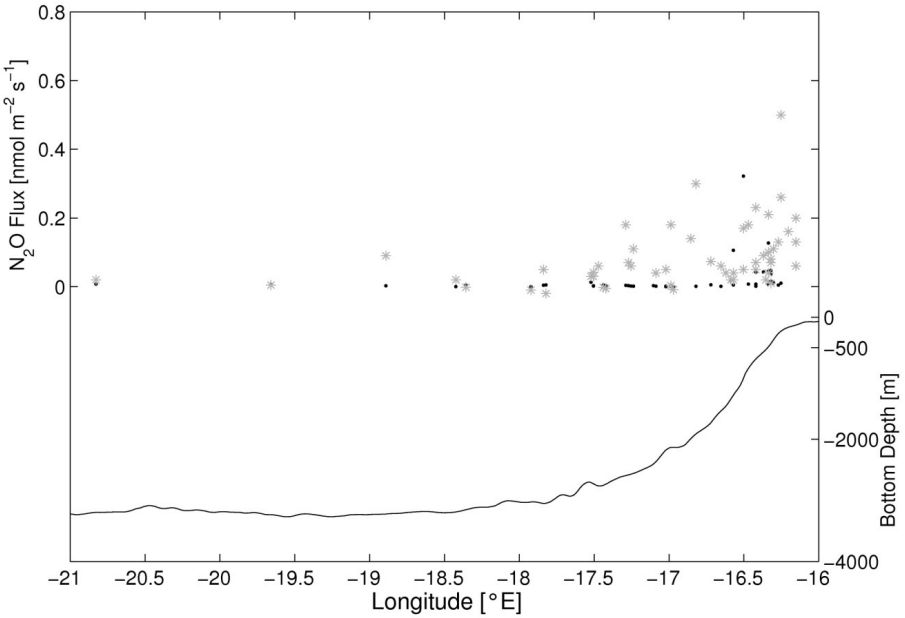

Fig. 2. Diapycnal N_2O (black dots, left axis) and air-sea fluxes (grey stars, left axis) projected to 18° N and bottom depth along 18° N (solid line, right axis). Fluxes from stations to the north and south of 18° N were projected onto 18° N according to their distance from the 400 m isobath.

BGD
8, 10229–10246, 2011

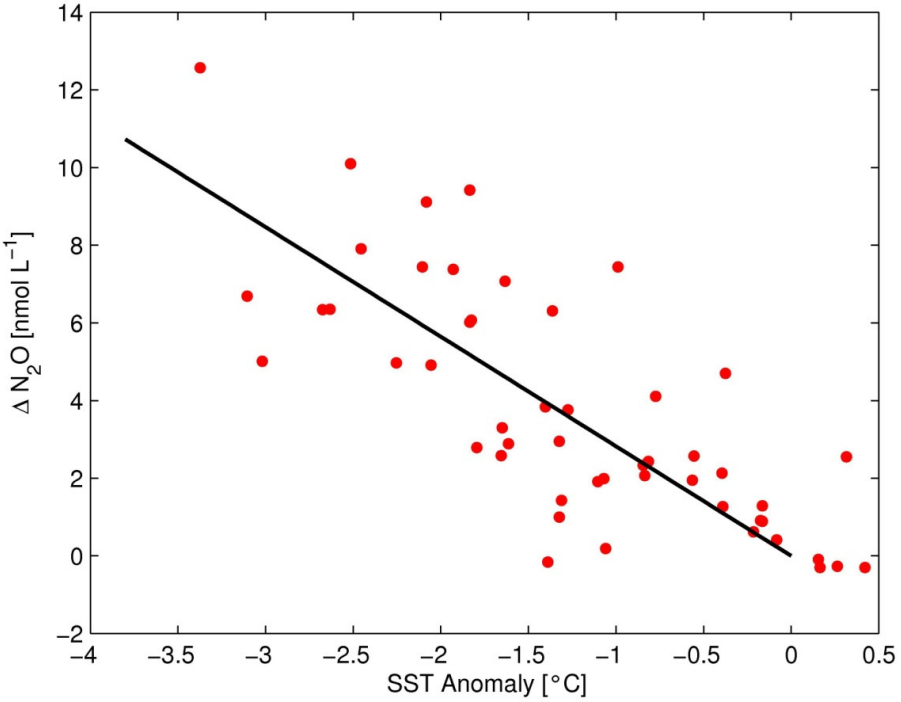

Fig. 3. ΔN_2O vs. SST anomaly. The black line denotes the linear regression of ΔN_2O with respect to the SST anomaly for SST anomalies smaller than zero.

BGD
8, 10229–10246, 2011

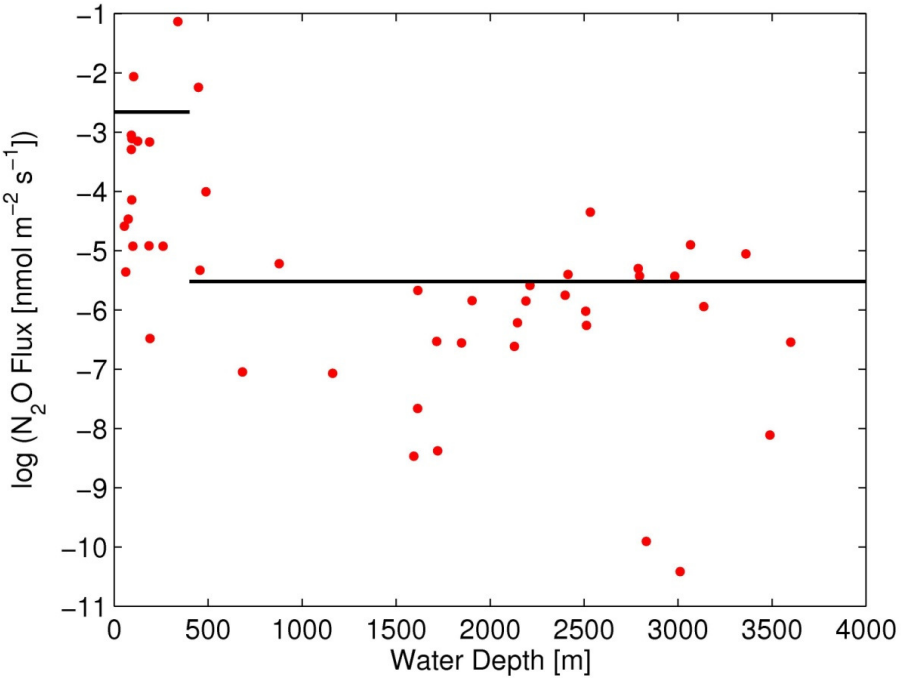

Fig. 4. Diapycnal N_2O fluxes vs. water depth. The black lines denote average fluxes for the shelf and for the open ocean region.

BGD
8, 10229–10246, 2011

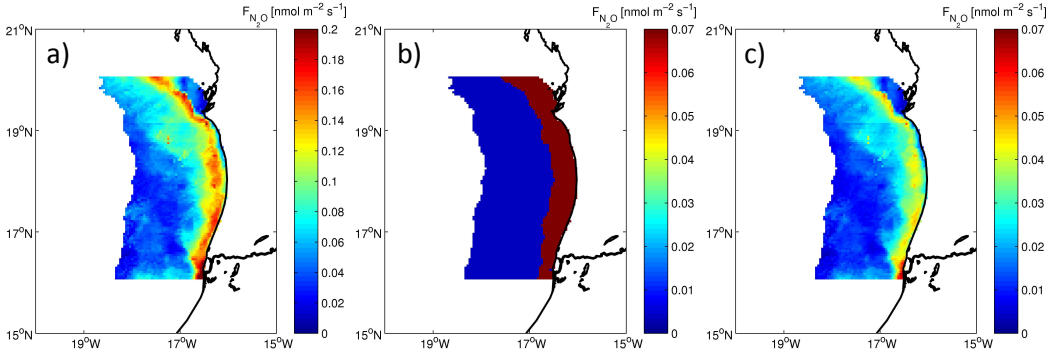

Fig. 5. (a) Regional distribution of the N_2O fluxes calculated from SST anomalies and averaged over the sampling time using the Nightingale (2000) parameterization. **(b)** Regional distribution of the diapycnal N_2O flux. **(c)** like **(a)** but using the Tsai and Liu (2003) parameterization. Please note the different scaling of the colorbars in **(a)** and **(b)**, **(c)**.

BGD
8, 10229–10246, 2011